NATIONAL AERONAUTICS AND SPACE ADMINISTRATION

Technical Memorandum 33-757

Performance of the Square Root Information Filter for Navigation of the Mariner 10 Spacecraft

C. S. Christensen

JET PROPULSION LABORATORY
CALIFORNIA INSTITUTE OF TECHNOLOGY
PASADENA, CALIFORNIA

January 15, 1976

PREFACE

The work described in this report was performed by the Mission Analysis Division of the Jet Propulsion Laboratory.

CONTENTS

Abstract

This report describes the use of a sequential least squares filter in the orbit determination for the Mariner Venus-Mercury (Mariner 10) spacecraft. The orbit determination strategy outlining the use of both the sequential filter and a conventional batch filter is given. Highlighted are the mission events from launch to the first Mercury encounter with emphasis on the sequential filter performance. Advantages to the mission derived from the sequential filter are pointed out.

Performance of the Square Root Information Filter for Navigation of the Mariner 10 Spacecraft

The flight of Mariner 10 was launched in November 1973. It encountered the planet Venus in February 1974, and the gravity assist of that flyby propelled the spacecraft towards Mercury. It encountered Mercury in late March 1974, and due to the 2:1 ratio of the spacecraft heliocentric period to that of Mercury, it was able to twice again encounter Mercury in September 1974 and in March 1975. At each of these four planetary encounters a wealth of scientific data was produced including thousands of closeup television pictures of the tiny planet Mercury.

One important ingredient in the success of this mission, the first spacecraft to achieve multiple planetary encounters, was highly accurate navigation. In performing the navigation, extensive use was made of a batch sequential filter and smoother, again, a first for interplanetary spacecraft navigation. This report will concentrate on the use of the batch sequential filter during the flight, the strategies followed, strengths and weaknesses of the filter, comparisons of the filter with a batch filter, and specific contributions to the mission from the filter.

Section I highlights characteristics of the mission and the premission analysis that led to the incorporation of the sequential filter into the mission software.

Section II gives the orbit determination strategy followed in using both a classical least squares constant parameters batch filter and the new sequential filter which is based on a process noise model; data sets, solutions sets, and choices of filter parameters are discussed.

Section III is a chronology of the mission navigation through the first Mercury encounter, highlighting the uses and advantages of the sequential filter.

Finally, in Section IV is a discussion of the payoffs derived from use of the sequential filter and some thoughts on its future use.

The mathematical basis for the design of the filter is given in Reference 1. The specific filter and smoother equations used in the Mariner 10 software are given in the Appendix.

I. Premission Analysis and Planning

An accuracy analysis study was conducted prior to the mission in order to determine the accurate capabilities of the orbit determination (O.D.) system. (see Reference 3). This study concentrated on the prime mission, i.e., up to the first Mercury encounter. The capability of subsequent Mercury encounters was considered, however.

It was clear from the analysis that the most critical period for orbit determination was the period determining the Venus encounter conditions. The reason for concern was the multiplication factor of approximately 1000 that existed between the Venus and Mercury aiming zone errors. This large factor was caused by the large gravity bending occurring at Venus encounter. This meant that a 1 kilometer error at Venus, if uncorrected, would result in about a 1000 kilometer error at Mercury.

Four trajectory correction maneuvers (TCM's) were planned: TCM1 at ten days after launch, to remove launch errors; TCM2 at 18 days prior to Venus encounter, to control the Venus encounter conditions; TCM3 at four days after Venus encounter, to remove Venus encounter errors; and TCM4 at 24 days after Venus encounter to remove errors introduced by the expected large TCM3 and to control the Mercury delivery. The orbit determination

prior to TCM2 was critical in assuring the accuracy of the Venus encounter.

Table I presents 1σ error ellipses in the Venus encounter plane derived from the O.D. during the long arc prior to TCM2. The table is composed of the major error sources and the associated position errors. Data noise represents the data quality of the doppler and range data*. The doppler noise is conservatively considered at 0.015 hz. (1σ) or equivalently 1 mm/sec for a 60 sec. count time, and range is considered at 50 meters (1σ). Ephemeris error, here, is the effect of the Venus position uncertainty relative to the earth at encounter time. Effective Station Location Errors (ESLE) includes uncertainties due to three factors.

1) The uncertainty of station locations on the earth's crust,
2) The uncertainty in the position of the earth's crust with respect to the earth's center (earth wobble), and
3) The uncertainty due to transmission effects - both in the earth's troposphere and ionosphere and charged particles in space (space plasma).

The troposphere changes the signal path length, and the charged particles change the group and phase velocity of the electromagnetic wave. All of these disturbances appear to, in effect, move the location of the tracking station.

The dominant error source as shown in Table I is the Non-Gravitational Acceleration (NGA) of the spacecraft. These accelerations are very small, typically on the order of 10^{-9} m/sec^2. Accelerations of this size would physically perturb the trajectory by only 3.5 kilometers in 30 days.

*Doppler and range data are defined and discussed in Section II.

However, the random time variations of the accelerations make their determination a difficult problem at best. The attitude control valves (2 for each axis) fire at various rates and leakage can be caused by improper valve seating due to dust particles, etc. Additionally, any unmodeled spacecraft configuration change can cause a change in solar pressure. The error shown in Table I is the result of modeling the NGA's as stochastic forces* and using a batch filter (which incorrectly assumes all parameters are constant over the entire data arc).

Table II presents the same information for the Mercury encounter. Again note the dominance of the nongravitational accelerations. The aiming zone or 'science success zone' at Mercury was about 500 x 200 km., so the predicted performance would meet that objective. Another reason for minimizing the Mercury flyby error was to fly close to the 'free return contour'** and minimize the fuel needed for a second Mercury encounter.

As a result of the preflight analysis leading to results such as those shown in Table I, the propellent tank size was doubled from a capability of 60 m/sec to a capability of 120 m/sec. Still, since about 1/3 m/sec would be needed at TCM3 to remove the error induced by each kilometer of miss at Venus, a 3σ error at Venus would have necessitated burning all of the propellent to correct the error induced and achieve the desired Mercury aim point. There would be no chance for a second Mercury encounter.

---

* The accelerations were modelled as constant over one day, exponentially correlated over time with a 3 day correlation time. The a priori uncertainties were: 0.5×10^{-9}, 1.75×10^{-9}, 3.0×10^{-9} m/sec^2 for the three axes.

** The free return contour was a locus of points in the Mercury aim plane such that an encounter passing through one of these points would have, after being perturbed by the planet, a heliocentric period exactly twice that of Mercury.

The batch sequential filter was designed and implemented in order to better model the NGA's and reduce the expected errors in the Venus delivery. The filter formulation makes use of the square root information estimation technology developed at the Jet Propulsion Laboratory and is described in the Appendix.

II. Orbit Determination Strategy

The primary data type used for outer space navigation is two-way doppler. A radio signal is transmitted from a station on the earth to the spacecraft and retransmitted to the same station (hence, two-way). Doppler data consists of a count of the difference between the number of cycles received and the number transmitted over a specified count interval (nominally, 1 minute). This gives a measure of the average topocentric (station centered) range rate over the count interval. Except for periods when the spacecraft is near a planet where gravitational acceleration is high, the doppler data can be averaged over a longer time (10 to 20 minutes) and still contain all the information necessary for orbit determination. This allows the information to be compressed into fewer data points.

A second data type, topocentric range, is obtained by measuring the time delay for a signal to travel round trip from the station to the spacecraft and return. Range data is complementary to doppler data in the sense that it has different information about the trajectory. Whereas doppler data was continuous, at the sample rates mentioned above, throughout the mission, range data was more sparse (typically one to three points during a station track of 8 - 10 hours, and there were many days with no range data).

Solutions were obtained using three data sets: doppler only, doppler and range, and range only. Consistency of the solutions based upon the different sets increased confidence in both the data and the solutions.

Different data arc lengths are sensitive to different error sources. ESLE effects and short term spacecraft leaks are much more important for short arcs (2-3 weeks or less). Long arcs are insensitive to ESLE effects, but can be degraded by long term spacecraft nongravitational forces. Hence whenever possible, solutions were obtained using data from both the longest arc available and a short arc (typically 20 days) containing the most recent data. By the longest arc available is meant data from the most recent large trajectory perturbation (e.g., a TCM) to the current time.

Orbit determination solutions were predicated upon a solution set based upon filter models with differing lists of parameters. This was done in order to assess the contributions of the various error sources as well as the continuing adequacy of the models. A basic consistency among the various solutions assured the latter. A solution set consisted of seven solutions estimating in turn.

a) The spacecraft state,

b) state + station locations,

c) state + solar pressure,

d) state + attitude control forces,

e) state + station location + solar pressure,

f) same as e) + attitude control,

g) all parameters.

Depending on the proximity to a planet, planetary or earth-moon mass and planetary and earth-moon ephemerides were included in g).

The solution set was run with two filters; the batch filter and the sequential filter. Both filters were mechanized using the numerically stable and accurate Householder orthogonal transformations. The mechanization is termed the Square Root Information Filter (SRIF). This mechanization is discussed in Reference 1 and more fully in Reference 5. The batch filter simply included all the data in a single batch. The sequential filter had a process noise model and was able to process sequentially at a fixed small batch size (cf Appendix).

The sequential filter was run with the three axis attitude control accelerations as colored noise stochastic parameters. A batch size of one day was used normally and correlation times of from one to five days were assumed. (The correlation time variation seemed to have little effect on the performance.) A priori sigmas of 10^{-9} m/sec^2 and 10^{-8} m/sec^2 were used.

Planetary targeting is usually expressed in terms of the B-plane. The B-plane (Reference 3) is a plane passing through the center of a target planet perpendicular to the incoming asymptote of a spacecraft. B·T is the intersection of the B-plane with the ecliptic and B·R is a vector in the B-plane perpendicular to B·T making a right handed system R, S, T where S is the incoming asymptote.

III. The Flight from Earth to Venus to Mercury

The flight path from Earth to Venus and to the first Mercury encounter is shown in Figure 1. Also shown is the location in the flight path of the three trajectory correction maneuvers.

When the spacecraft was within the strong gravity field of the Earth, its orbit was determined rather quickly compared to the time required in

interplanetary space. One day after launch when tracking stations around the Earth had supplied tracking data, a reasonable O. D. was obtained. This fit was updated over the next few days and used to plan TCM1 at launch plus 10 days.

Using doppler and range data, the one sigma error ellipse in the Venus B-plane was about 400 km by 200 km. This was small compared to the TCM1 execution one sigma error of 1500 km. The batch filter and sequential filter performance was similar in this phase due to the strong near Earth data and the short time span.

The mission phase from TCM1 to TCM2 was the most critical for orbit determination. The accuracy of the orbit determined the parameters for TCM2 which in turn determined the Venus delivery accuracy. Due to the geometry of the swingby trajectory there was a 1 to 1000 mapping of errors from Venus to Mercury. In other words, a one kilometer miss at Venus mapped into a one thousand kilometer miss at Mercury.

A time history of solutions in the Venus B-plane is shown in Figure 2 for batch filter solutions, and in Figure 3 for sequential filter solutions. Solutions for both long and short data arcs are shown for doppler only and doppler + range. The long data arc is from TCM1 (11/13/73) to the date shown on the abscissa. The short data arc is the 20 days preceding the date shown on the abscissa. All solutions shown include the spacecraft state, solar pressure parameters, and station locations. This solution set was chosen as representative; other solution sets show similar behavior. Note that all of the fits with data up to 12/24 showed good agreement. The batch filter fits with data up to 1/2, however, show a wide scatter in B·R. One week later with data up to 1/10 the wide scatter is apparent in both B·R and B·T with the short arc doppler solution 800 km high in B·R. The sequential

filter, on the other hand, with the exception of a short arc solution high in B·R, remained remarkably flat throughou. :he entire time period.

Some insight into the scatter of solutions shown in Figure 2 and the apparent stability of the sequential filter solutions in Figure 3 can be gained from examining Figure 4. This figure is a plot of the spacecraft nongravitational accelerations as represented by the magnitude of the smoothed solution vector for the attitude control accelerations. Of course, this is simply the acceleration that the filter sees, i.e., that along the Earth-spacecraft line of sight. The filter parameters were: one day batch size, 5 day correlation times, and a priori sigmas of . x 10^{-9} m/sec^2 along each axis.

Significant peaks in Figure 4 are numbered. Peak Nos. 1, 2 and 3 occur on days when roll calibrations were performed. The spacecraft was allowed to roll about the spacecraft - sun axis at a rate of 40 min/rev for 6 revs. This meant that for 4 hours the solar pressure component perpendicular to the sunline was averaged out, so the average acceleration due to this component was less for the day. When it was first noticed that the sequential filter was sensitive to this minute force, the Navigation Team members were surprised and gratified that the filter and the model were performing so well.

Peak No. 4 occurred on January 4. This unusually high acceleration shown by the filter was confirmed by a ramp in the doppler residuals beginning on January 4 and lasting for about a day. The total doppler shift was about -0.01 hz. corresponding to a velocity change of 0.6 mm/sec. Subsequent analysis of telemetered limit cycle data indicated a pitch axis torque lasting for about 25 hours on January 4 and 5. It was calculated that a valve leak

large enough to cause the observed torque and the observed velocity change would have been less than 0.9 grams of gas expended. This is too small to be detected by the gas consumption telemetry.

Here is an example of a spacecraft nongravitational force (a gas leak) too small to be seen by telemetry but large enough to effect the orbit determination (the scatter of solutions shown in Figure 2). The sequential filter modelled the disturbance beautifully and provided a stable Venus B-plane solution to use in the determination of the parameters for TCM2.

Peaks 5 and 6 have no easy explanation. Peak 5 is probably a filter induced damping to fit of peak 4 and peak 6 is probably another spacecraft leak.

After TCM2, O.D. solutions were made every two days in order to get a rapid determination of the trajectory. Had TCM2 not been successful there was still time to do another maneuver prior to the Venus encounter. Here the batch and sequential filter gave similar results over the one week period. Figure 5a shows the solutions in the Venus B-plane for 3, 5 and 7 day arcs.

On January 28, one week before Venus encounter, the spacecraft developed a serious problem. The roll gyros began oscillating at a rapid rate, causing the roll position jets to fire at their maximum rates. The immediate effect was a large consumption of cold nitrogen used as attitude control gas (0.54 kg. in 79 minutes) before the problem was diagnosed and the gyros turned off. The thrust imbalance in the attitude control jets imparted a force on the spacecraft. The doppler pseudoresiduals* indicated a doppler shift of 0.13 hz. or a radial velocity change of 8.5 mm/sec in 79 minutes,

*observed-computed values

hence the radial acceleration was 1.79×10^{-6} m/sec^2. This was a large enough acceleration to have two effects: 1) the O.D. data arcs had to be restarted, and 2) the trajectory was changed thus altering the Venus B-plane position. It was suspected that at the time that the unseen component of the acceleration vector could have been large enough to move the trajectory up to 100 km in the Venus B-plane. That size error at Venus would have seriously degraded the science return at Mercury.

After the gas acceleration on January 28, short arc fits were again made every two days. Figure 5b shows these solutions for 3, 5 and 7 days. Also shown is the actual trajectory point determined after the Venus flyby.* By comparing these solutions with those of the previous week, it is seen that the January 28 acceleration moved the trajectory only about 15 km in the B-plane. This number is consistent with that obtained postflight by solving for the acceleration and analyzing the spacecraft telemetry giving gas usage and torques.

Also shown in Figure 5 is the desired aim point and the actual aim point. These are different because the spacecraft had discrete turn and burn time capabilities. The actual aim point was the closest realizable aim point to the desired point. The proximity of the flyby point to the desired aim point (17 km) is remarkable. It is much smaller than the preflight statistics shown in Table I indicated. This was fortuitous in that, because of the small miss, a large TCM shortly after Venus encounter was not necessary. Further the direction of the miss was such that the

---

* to the large Venus gravity field experienced approaching and leaving planet, the state of the spacecraft was determined very accurately within less than 1 km in the Venus B-plane).

desired Mercury aim point could be achieved with a 'sunline'* TCM on March 16.

On February 14 the gyros were turned on in order to test the conditions under which the January 28 failure had occurred. The oscillations again appeared and another spacecraft acceleration resulted (1.75×10^{-6} m/sec^2 for 20 min.). It was then decided not to attempt a full maneuver but to use the sunline TCM on March 16.

Figure 6 is a continuation of Figure 4 showing the radial nongravitational acceleration from TCM1 through the Mercury encounter. It was constructed by joining 5 different O.D. fits (data arcs starting at each TCM and at the large anomalies of January 28 and February 14). Two additional peaks are noted. Peaks marked 7 and 8 on days 107 and 123 correspond to 'flyback and sweeps' where the reference star was lost and attitude control gas was expended in the reacquisition search. It is seen that the level of the spacecraft nongravitational accelerations is generally higher after the January 4 peak.

An example of the effect of this high level on the batch filter can be seen in Figure 7 which shows various O.D. solutions in the Mercury B-plane. The solutions labelled 1 contain data only near Venus encounter (February 4). The solutions labelled 2 and 3 contain data starting after the February 14 leak (day 103). The batch filter solutions are badly scattered whereas

*The engine nozzle pointed toward the sun in the normal spacecraft cruise attitude, so if the engine is fired with no turns, the thrust vector imparted to the spacecraft is along the sun-spacecraft line, hence the name 'sunline'. Rather than three degrees of freedom, the sunline maneuver only has two: the magnitude of the thrust and the time the maneuver takes place. The advantage of a sunline maneuver was that the gyros needed only be turned on for the few seconds during which the engine fired, rather than the hour or so needed for a full maneuver with turns.

the sequential filter solutions cluster relatively tightly. The scatter of the batch filter solutions can be attributed to its inability to model the high level of nongravitational accelerations. The data spans for solutions 2 and 3 are indicated in Figure 6. It is seen that solution 2 contains peak 7 and solution 3 contains both peaks 7 and 8. As with TCM2, the best orbit used to determine the TCM3 parameters was given by the sequential filter.

After TCM3 the primary purpose of orbit determination was to accurately determine the trajectory so that the science instruments could be pointed accurately. The Mercury flyby was about 160 km from the aim point, well within the science success zone.

The spacecraft was now in an orbit about the sun with a period twice that of Mercury. This enabled two more Mercury encounters, one in September 1974 and one in March 1975 before the spacecraft attitude control gas was depleted. The sequential filter was used as well as the batch filter throughout the remainder of the mission. The performance differential of the two filters, however, was not as dramatic as that in the early mission described above. Some navigation results of the extended mission are given in References 4 and 6.

IV. Conclusions

The performance of the square root mechanized batch-sequential filter in the navigation of Mariner 10 was impressive. It demonstrated that the SRIF formulation is a viable one for use in mission operations and also that a first order colored noise model adequately described the NGA effects.

The sequential filter was heavily used and relied upon during the mission. It is difficult to say what would have transpired had it not been available, or a different filter mechanization used but it is quite conceivable that a less accurate O.D. during the critical pre-Venus phase would have caused a large change in the remainder of the mission. Though the direction of the error at Venus was fortuitous in that a sunline maneuver was possible to obtain the desired Mercury delivery, a large error at Venus would have severely degraded the Mercury delivery. This, in turn, would have not only degraded the science return on the first Mercury encounter, but could have precluded any further Mercury encounters.

Based on the success indicated here, the square root sequential filter with process noise is now a tested, accepted tool for interplanetary orbit determination. Essentially the same filter with some added capabilities (e.g., variable batch sizes, ability to model white noise as well as colored noise, smoothed covariances, and smoothed sensitivities will be used in the upcoming Viking mission to Mars. This state-of-the-art estimation mechanization is described in Reference 1.

Table I

Venus Preencounter Error Budget

Error Source	1 Sigma Error Ellipse in the B-plane (km) SMAA		SMIA
1. Data Noise	18	x	2
2. Ephemeris	9	x	5
3. ESLE	38	x	5
4. NGA	93	x	22
5. Total	99	x	36

(SMAA - semimajor axis, SMIA - semiminor axis)

Table II

Mercury Preencounter Error Budget

Error Source	1 Sigma Error Ellipse in the B-plane (km) SMAA		SMIA
1. Data Noise	10	x	7
2. Ephemeris	65	x	42
3. ESLE	20	x	8
4. NGA	159	x	120
5. Total	172	x	129

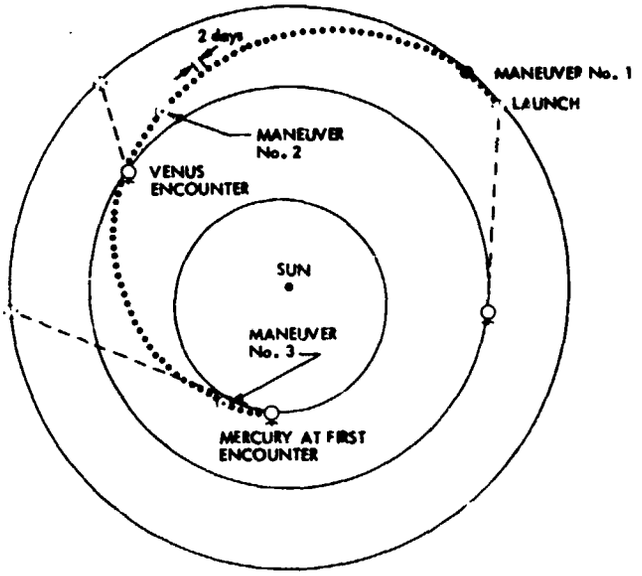

Fig. 1. Projection of the Earth to Mercury trajectory into the ecliptic plane

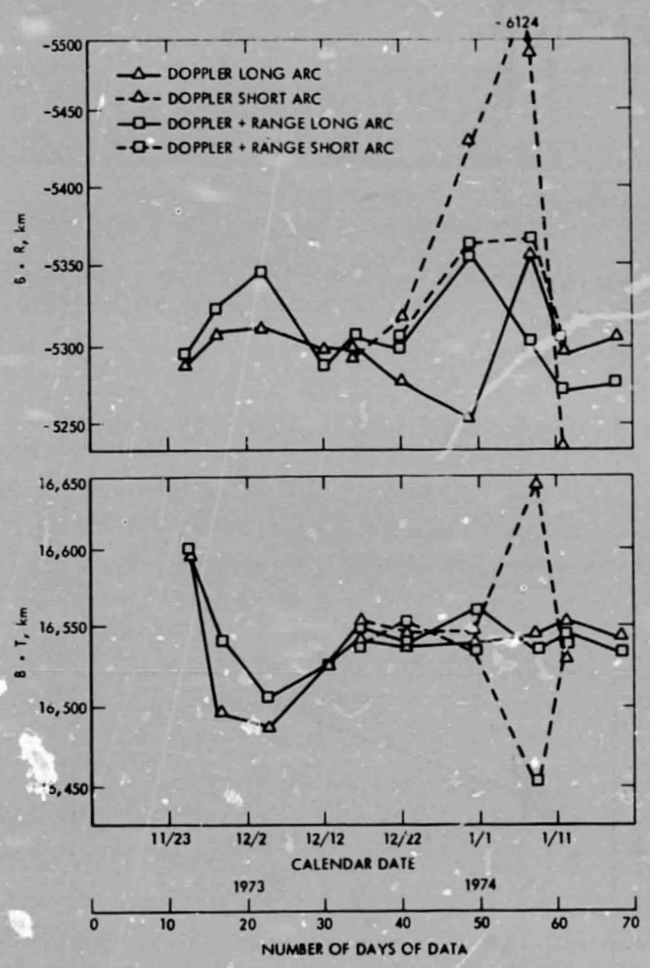

Fig. 2. Time history of solutions in the Venus B-plane: batch filter

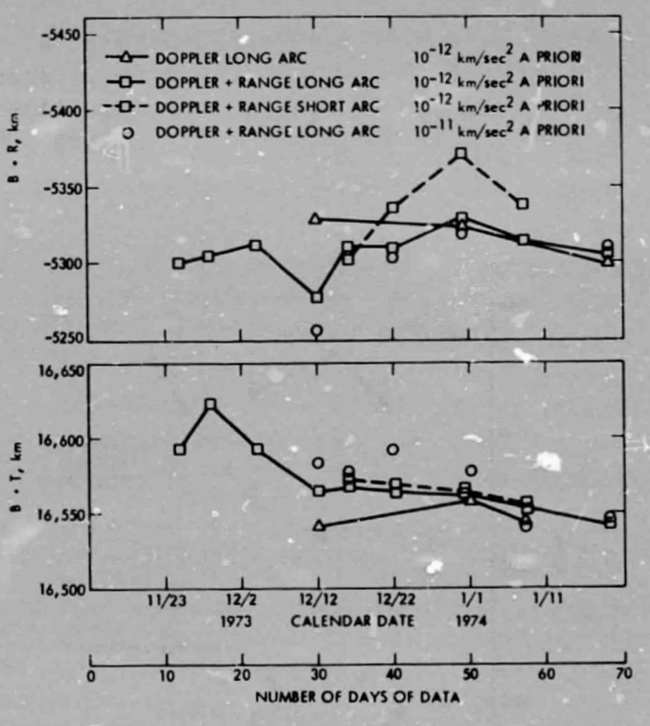

Fig. 3. Time history of solutions in the Venus B-plane: sequential filter

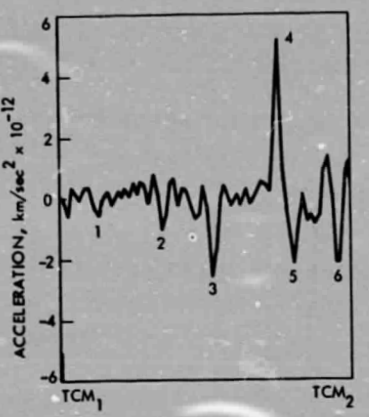

Fig. 4. Spacecraft accelerations along the line of sight between TCM_1 and TCM_2

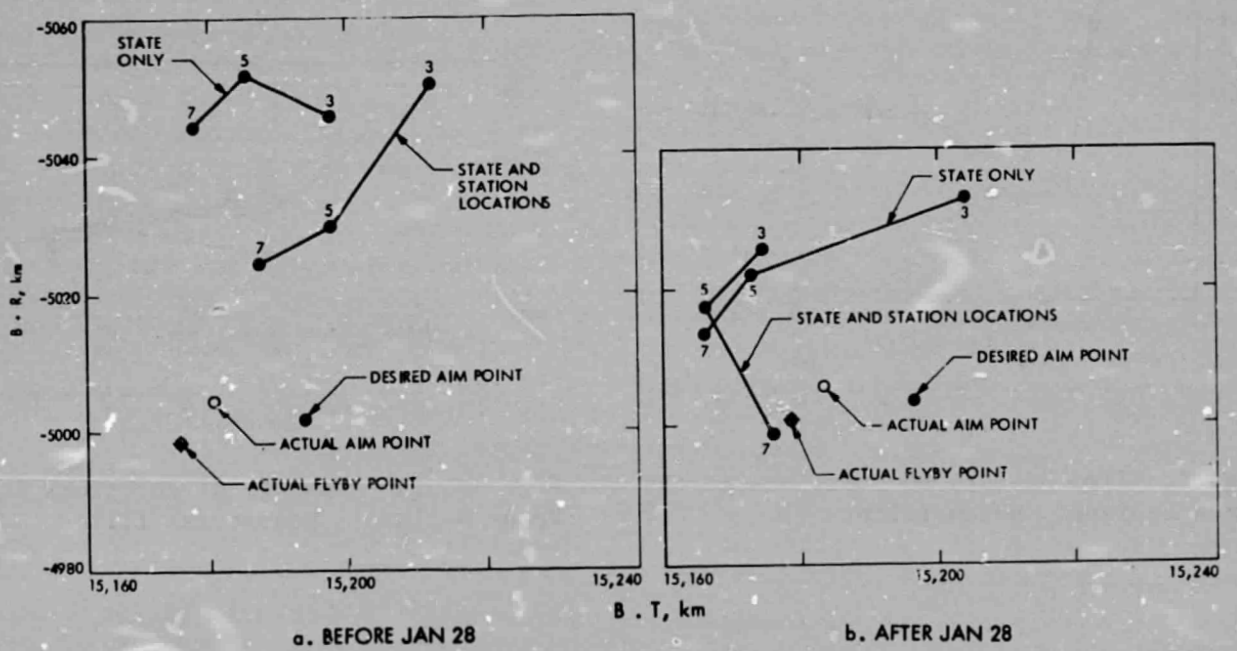

Fig. 5. Venus approach short arc solutions

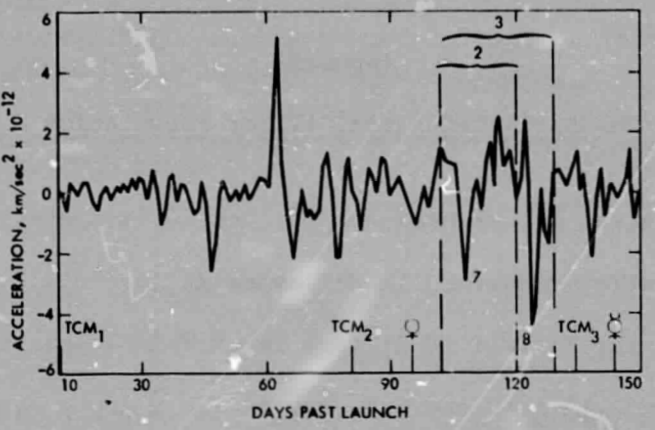

Fig. 6. Spacecraft accelerations along the line of sight

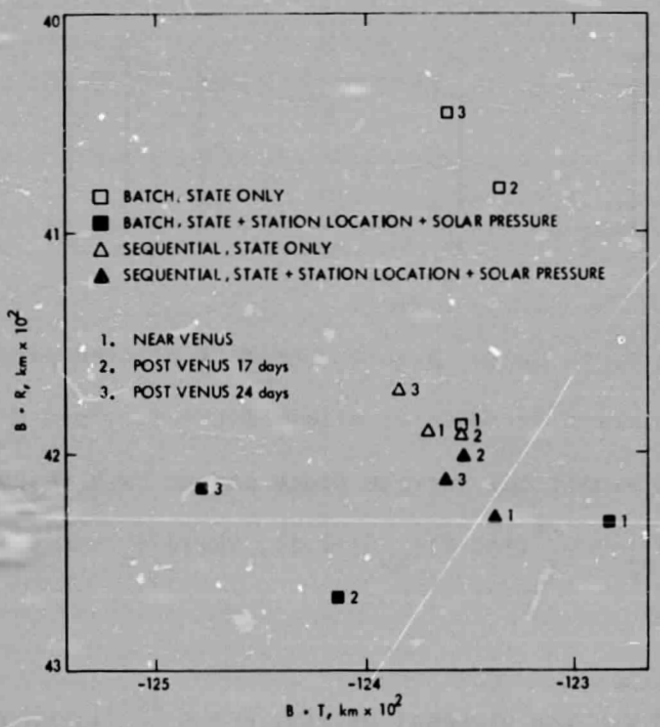

Figure 7. Batch filter vs sequential filter in the Mercury B-plane

Appendix

The Batch-Sequential Filter Formulation

The sequential filter used for Mariner 10 is a precursor to the filter mechanization described in Reference 1, Appendix B. The filter formulation for the Mariner 10 differs in certain respects from that given in Reference 1, e.g. the ordering of the $\bar{x}$ and p equations and the necessity for a nonsingular M. For completeness the formulation of the Mariner 10 filter is given here in brief outline; for more detail see References 1 and 2.

The system dynamics are:

$$\begin{bmatrix} \bar{x} \\ p \\ y \end{bmatrix}_{j+1} = \begin{bmatrix} I & V_{pj} & 0 \\ 0 & M & 0 \\ 0 & 0 & I \end{bmatrix} \begin{bmatrix} \bar{x} \\ p \\ y \end{bmatrix}_{j} + \begin{bmatrix} 0 \\ w_{j+1} \\ 0 \end{bmatrix} \qquad \text{A.1}$$

where $\bar{x}$ is the epoch state, p is a vector of colored process noise, y is a vector of constant parameters, w is white noise, and M is a nonsingular matrix.* $\bar{x}$ is simply the current state mapped back to epoch without process noise; hence $V_{pj} = \phi_x^{-1}(j+1,0)\phi_{xp}(j+1,j)$, where ϕ_x and ϕ_{xp} are transition matrix elements.

*In practice M was the diagonal matrix, $M = e^{-\Delta t/\tau} I$, where Δt is the batch size, τ the correlation time, and I is the identity matrix. Hence the stochastic parameters are uncorrelated from each other but each is correlated in time.

Data is accumulated in the first batch; a priori statistics on $\bar{x}$ and p are added; and a Householder triangularization is performed to obtain the data equation

$$\begin{bmatrix} R_x & R_{xp} & R_{xy} \\ 0 & R_p & R_{py} \\ 0 & 0 & R_y \end{bmatrix}_j \begin{bmatrix} \bar{x} \\ p \\ y \end{bmatrix}_j = \begin{bmatrix} z_x \\ z_p \\ z_y \end{bmatrix} - \begin{bmatrix} \nu_x \\ \nu_p \\ \nu_y \end{bmatrix} \qquad \text{A.2}$$

To map from j to j+1 simply solve Equation A.1 for $\begin{bmatrix} \bar{x} \\ p \\ y \end{bmatrix}_j$

yielding

$$\begin{bmatrix} \bar{x} \\ p \\ y \end{bmatrix}_j \begin{bmatrix} V_{pj}M^{-1} & I & -V_{pj}M^{-1} & 0 \\ -M^{-1} & 0 & M^{-1} & 0 \\ 0 & 0 & 0 & I \end{bmatrix} \begin{bmatrix} w \\ \bar{x} \\ p \\ y \end{bmatrix}_{j+1} \qquad \text{A.3}$$

Substituting (A.3) into (A.2) and adding the a priori statistics on w_{j+1} yields on the left hand side of the data equation

$$\begin{bmatrix} R_x V_{pj} M^{-1} - R_{xp} M^{-1} & R_x & -(1,1) & R_{xy} \\ -R_p M^{-1} & 0 & R_p M^{-1} & R_{py} \\ 0 & 0 & 0 & R_y \\ \Lambda_w^{-\frac{1}{2}} & 0 & 0 & 0 \end{bmatrix} \begin{bmatrix} w \\ \bar{x} \\ p \\ y \end{bmatrix}_{j+1}$$

where the (1,3) term is the negative of the (1,1) term as indicated.

A Householder transformation is performed to obtain

$$\begin{bmatrix} R'_w & R'_{wx} & R'_{wp} & R'_{wy} \\ 0 & R'_x & R'_{xp} & R'_{xy} \\ 0 & 0 & R'_p & R'_{py} \\ 0 & 0 & 0 & R'_y \end{bmatrix} \begin{bmatrix} w \\ \bar{x} \\ p \\ y \end{bmatrix}_{j+1} = \begin{bmatrix} z'_w \\ z'_x \\ z'_p \\ z'_y \end{bmatrix} - \begin{bmatrix} \nu'_w \\ \nu'_x \\ \nu'_p \\ \nu'_y \end{bmatrix} \qquad \text{A.4}$$

where primes denote the new values.

Now, the upper row of (A.4) is saved for smoothing. The remaining three rows are augmented by data in the j+1st batch and triangularized again by a Householder process. This equation then replaces (A.2) and the process repeats.

In order to obtain equations for smoothed estimates, the first row of (A.4) is solved for w (assuming zero estimate for the data equation noise) to obtain:

$$w^*_{j+1} = -R'^{-1}_w \left[R'_{wx} \bar{x}^*_{j+1} + R'_{wp} p^*_{j+1} + R'_{wy} y^* - z'_w \right]$$

From (A.1)

$$p_j^* = M^{-1}(p^*_{j+1} - w^*_{j+1})$$

or $$p_j^* = M^{-1}\left[(I + R'^{-1}_w R'_{wp}) p^*_{j+1} + R'^{-1}_w R'_{wx} \bar{x}^*_{j+1} + R'^{-1}_w R'_{wy} y^* - R'^{-1}_w z'_w\right] \qquad \text{A.5}$$

Also from (A.1)

$$\bar{x}^*_j = \bar{x}^*_{j+1} - v_{pj} p^*_j \qquad \text{A.6}$$

Equations (A.5) and (A.6) form a backwards recursion for $\bar{x}^*$ and p^* that, if started with the final filtered estimates (which are, by definition, smoothed estimates), yield smoothed estimates for each batch.

References

1. Bierman, G. ., "Sequential Least-Squares Using Orthogonal Transformations", TM 33-735, Jet Propulsion Laboratory, Pasadena, Calif., August 1975.

2. Christensen, C. S., "A New DPODP Sequential Filter", MOS SRD 73-3-482/c (internal document), Jet Propulsion Laboratory, Pasadena, Calif., 1971.

3. Christensen, C. S., et al., "Final Orbit Determination Strategy and Accuracy, Mariner Venus-Mercury 1973", Project Document 615-128 (internal document), Jet Propulsion Laboratory, Pasadena, Calif., July 1973.

4. Christensen, C. S., Reinbold, S. J., "Navigation of the Mariner 10 Spacecraft to Venus and Mercury", Journal of Spacecraft and Rockets, Vol. 12, No. 5, May 1975, pp. 280-286.

5. Lawson, C. L., Hanson, R. J., Solving Least Squares Problems, Prentice-Hall Englewood Cliffs, New Jersey, 1974.

6. Bantell, M. H., and Jones, J. B., "Navigation Results of the Mariner Venus/Mercury 1973 Mission", AIAA Paper No. 75-84, AIAA Aerospace Science Meeting, Pasadena, California, January 1975.